Evaluation of Credit Value Adjustment in K-forward

Xuemiao Hao[*], Chunli Liang[†], Linghua Wei[‡]

April 27, 2017

Abstract

We model and quantify counterparty credit risk for K-forward, a newly proposed longevity-linked security. We focus on the evaluation of credit value adjustment (CVA) from the longevity risk hedger's perspective. The modeling involves two folds. First, we use a vector autoregressive integrated moving-average process to model the time series of mortality indexes that is obtained by applying the original Cairns–Blake–Dowd model. Then, the risk-neutral default probability of the hedge provider is obtained by calibrating a reduced-form default model on the market price of bonds issued by the hedge provider. We calculate and compare CVA in K-forwards for different combinations of hedger provider, reference year and recovery rate.

Keywords: credit value adjustment; K-forward; longevity risk
JEL Classification: C13, C15, G22

1 Introduction

Mortality in many countries has been steadily improving for decades thanks to medical improvement and stable social environment. This trend makes longevity risk the main problem that pension funds face nowadays. A new market, the life market, has come into form over the last decade, in which mortality- and longevity-linked securities are traded (Blake *et al.*, 2013). These new products are welcomed by financial market since they could add more diversity to traditional capital market. For instance, longevity risk can be transferred to broader capital market through various securities, such as longevity bond (Blake *et al.*, 2006; Hunt and Blake, 2015), longevity swap (Cairns *et al.*, 2014), and

[*]Corresponding author. Asper School of Business, University of Manitoba, Winnipeg, Manitoba R3T 5V4, Canada. E-mail: `xuemiao.hao@umanitoba.ca`; tel: +1-204-474-8710; fax: +1-204-474-7545.

[†]Asper School of Business, University of Manitoba, Winnipeg, Manitoba R3T 5V4, Canada. E-mail: `liangc3@myumanitoba.ca`.

[‡]Asper School of Business, University of Manitoba, Winnipeg, Manitoba R3T 5V4, Canada. E-mail: `weil@myumanitoba.ca`.

q-forward (Coughlan *et al.*, 2007). For all these securities, the payoff is designed to be linked to the mortality rates of some reference populations at some reference years in the future.

More recently, Chan *et al.* (2014) and Tan *et al.* (2014) proposed a simple longevity-linked security called K-forward to hedge longevity risk. A K-forward is a zero-coupon swap that exchanges on the maturity date some fixed amount for a floating amount that is proportional to a mortality index in the Cairns–Blake–Dowd (CBD) mortality model for a certain population. Figure 1 shows the payoffs on the maturity date of a typical K-forward. The longevity-risk hedger plays the role as the fixed rate receiver and the hedge provider as the fixed rate payer in this contract. If the mortality index turns out to be lower than expected and thus there is a longevity loss, the hedger will get a positive payment from the hedge provider to cover the loss. Compared with other longevity hedging instruments, a big advantage of K-forwards is that their final payoffs only depend on some time-varying mortality index and there is no need to specify a specific hedging age. This feature makes a K-forward longevity hedge easier to implement and thus more conductive to the development of liquidity.

Figure 1 is here.

Like other longevity-linked securities, K-forward is supposed to be traded over the counter. Thus, it is necessary to measure its counterparty risk. However, very few papers in the literature have studied counterparty risk in longevity-linked securities until recently Biffis *et al.* (2016) investigated the cost of bilateral default risk and collateral rules in longevity swaps. In particular, they assumed that the credit risk of the hedge supplier is equal to the average credit quality of the LIBOR panel and thus its default intensity follows the LIBOR-Treasury spread. In this paper, we propose a framework to evaluate credit value adjustment (CVA) in K-forwards. One advantage of our work is that we are able to estimate the risk-neutral default intensity for an arbitrary hedge supplier given that we can collect enough market information, like corporate bonds, reflecting its credit risk. For simplicity, we consider a K-forward contract without collateral requirements. Also, since the mortality index data is available once a year, we assume that the evaluation of the K-forward can be done only at the end of each year after the mortality index data for that year is available. The CVA at time 0 can be approximated as follows:

$$\mathrm{CVA} \approx (1-R)\sum_{t=1}^{T} \mathrm{DF}(t)\cdot \mathrm{EE}(t)\cdot (F(t)-F(t-1)), \tag{1.1}$$

where $1-R$ is the loss given default (LGD), which is the percentage of the exposure to be lost at default of the counterparty, $\mathrm{DF}(t)$ is the risk-free discount factor for time t, $\mathrm{EE}(t)$ is the expected risk exposure for the institution at time t, and $F(t)$ is the counterparty's risk-neutral default probability by time t. See Gregory (2015; Appendix 14) for the detailed derivation of formula (1.1).

We want to point out some important underlying assumptions for the plausibility of using formula (1.1) to evaluate the counterparty risk in K-forward. First, the recovery rate is assumed to be exogenously given and fixed. Second, we consider the possible default of the hedge provider only and ignore the possibility that the hedger may also default. This assumption may seem unrealistic at first glance. But if we think of the hedger as a pension fund, whose default is mainly due to unexpected improved mortality rate, we would agree that when the hedger's default risk is high the risk exposure to the hedge provider is likely to be zero. Last, we assume that there is no wrong-way or right-way risk, i.e., the credit risk exposure is independent with the hedge provider's default time. This assumption is reasonable since banks usually do not have exposures to the demographics of a population. Based on these assumptions, we can simply accumulate over time the product of the LGD, the risk exposure and the default probability to evaluate the counterparty risk as in formula (1.1).

Another important issue we want to address regarding formula (1.1) is that we calculate the expected risk exposure under the real-world measure. Usually, since evaluation of CVA is a pricing application, the expected risk exposure should be calculated under the risk-neutral measure instead of the real-world measure. However, there is essentially no publicly available pricing information on longevity-linked securities with the only exception for the longevity bond by the European Investment Bank (EIB) in 2004. While the EIB longevity bond had an issue price of 35 basis points below LIBOR, it was ultimately unsuccessfully issued. The lack of real pricing information makes it impossible to derive reliable risk-neutral mortality indexes. It is also the reason why Biffis *et al.* (2016) assumed that the death time has the same intensity process under both risk-neutral and real-world measures. We further want to point out that, as Cox and Pedersen (2000) explained for catastrophe risks, if a future cash flow depends only on mortality related variables, which are assumed independent of financial risk variables, then the cash flow's expectation under the risk-neutral measure coincides with that under the real-world measure. Hence, in this paper we derive the CBD mortality indexes under the real-world measure and use them to calculate the expected risk exposure at each time t, which is consistent with market practice where counterparties would agree on a real-world mortality model.

The remaining of the paper is organized as follows. In Section 2, we derive the CBD mortality index data for a reference population and fit it by using a vector time-series model. The time-series model is used to predict future mortality indexes for the population. In Section 3, we estimate the risk-neutral default probability by calibrating a reduced-form default model on market price of bonds. Then, combining results in Sections 2 and 3, we calculate the CVA in K-forwards for two potential hedge providers in Section 4. Some concluding remarks are given in Section 5.

2 Model for mortality indexes

The multiperiod-ahead forecasting performance of a stochastic mortality model is essential to its application in longevity risk management. From the work of Cairns *et al.* (2011) and Dowd *et al.* (2010), we know that the original CBD mortality model (Cairns *et al.*, 2006) is a relatively simple one among a few that can provide acceptable both ex ante and ex post forecasts, in particular, for senior ages. Recall that the reparameterized version of the original CBD two-factor mortality model assumes that

$$\ln\left(\frac{q_{x,t}}{1-q_{x,t}}\right) = \kappa_t^{(1)} + \kappa_t^{(2)}(x-\overline{x}), \tag{2.1}$$

where $q_{x,t}$ is the probability that an individual aged x at time t will die by $t+1$, $\overline{x}$ is the average of the ages used in the dataset, and $\kappa_t^{(i)}, i = 1,2$, called CBD mortality indexes, are time-varying parameters representing period effects. Assuming deaths follow a binomial distribution one can estimate $\kappa_t^{(1)}$ and $\kappa_t^{(2)}$ using historical mortality rates. Note that $\kappa_t^{(1)}$ represents the level of the logit-transformed mortality curve and a reduction in $\kappa_t^{(1)}$ means an overall mortality improvement. $\kappa_t^{(2)}$ represents the slope of the logit-transformed mortality curve and a positive $\kappa_t^{(2)}$ means that mortality at older ages improves more slowly than at younger ages.

Chan *et al.* (2014) pointed out a unique feature, the so-called new-data-invariant property, of the CBD mortality indexes. In other words, after new mortality data is available and the CBD model (2.1) is updated accordingly, historical values of $\kappa_t^{(i)}, i = 1,2$, will not change. This is a very important property based on which Chan *et al.* (2014) proposed the concept of K-forward. A K-forward could be considered as a zero coupon swap that exchanges a fixed amount with a floating amount proportional to $\kappa_T^{(1)}$ or $\kappa_T^{(2)}$ for a reference population in a future reference year T. Denote by $\tilde{\kappa}_T^{(i)}$ the forward mortality index, which is determined at time 0, and by Y the notional amount. The payoff for the fixed rate receiver on the maturity date can be expressed as

$$Y \cdot \left(\tilde{\kappa}_T^{(i)} - \kappa_T^{(i)}\right), \qquad i \in \{1,2\}. \tag{2.2}$$

2.1 Mortality data

The mortality data used in this paper is that for US males aged from 30 to 100. The reason why we choose the age range 30–100 has two folds. First, we want to exclude the accident hump at younger ages for which the CBD model does not handle well. Second, the average age is 65, the normal age at which people retire in US. So if $\kappa_T^{(2)}$ is lower than $\tilde{\kappa}_T^{(2)}$ then it would result in extra longevity risk from all retiree groups. Human Mortality Database (2016) has mortality data for US males from 1933 to 2014. Although a structural change should have occurred during this period, see Li *et al.* (2011), we still use all available mortality data for a baseline case in this paper. The historical values of $\kappa_t^{(1)}$ and $\kappa_t^{(2)}$ are shown in Figure 2.

Figure 2 is here.

2.2 Vector time-series model

In the original CBD model the time variation of $\boldsymbol{\kappa}_t = (\kappa_t^{(1)}, \kappa_t^{(2)})^\mathsf{T}$ is modeled by a bivariate random walk (Carins *et al.*, 2006). However, a random walk cannot explain either serial or cross correlation in the series of $\Delta\boldsymbol{\kappa}_t = \boldsymbol{\kappa}_t - \boldsymbol{\kappa}_{t-1}$, though such correlations are significantly observed for almost all populations available. Chan *et al.* (2014) proposed to apply a vector autoregressive moving-average (VARMA) model on $\Delta\boldsymbol{\kappa}_t$ and found the best fitting VARMA model for England and Wales male population from 1950 to 2009. Following Chan *et al.* (2014), we find in this section the best VARMA model describing the CBD mortality indexes for US male population from 1933 to 2014.

Let us denote $\Delta^d\boldsymbol{\kappa}_t = \Delta^{d-1}\boldsymbol{\kappa}_t - \Delta^{d-1}\boldsymbol{\kappa}_{t-1}, d \geq 1$, with $\Delta^0\boldsymbol{\kappa}_t = \boldsymbol{\kappa}_t$. We say that the vector series $\Delta^d\boldsymbol{\kappa}_t$ follows a VARMA(p,q) process if

$$\Delta^d\boldsymbol{\kappa}_t = \Phi_0 + \sum_{i=1}^{p} \Phi_i \Delta^d \boldsymbol{\kappa}_{t-i} - \sum_{j=1}^{q} \Theta_j \boldsymbol{\epsilon}_{t-j} + \boldsymbol{\epsilon}_t, \tag{2.3}$$

where Φ_0 is a constant vector, Φ_i's and Θ_j's are coefficient matrices for $i, j \geq 1$, $\Phi_p \neq 0$, $\Theta_q \neq 0$, and $\boldsymbol{\epsilon}_t$ is a sequence of independent and identically distributed random vectors with mean zero and positive-definite covariance matrix Σ. It is known that for a VMA(q) process its cross-correlation matrices with lag $> q$ are all zero and for a VAR(p) process its partial autoregressive matrices with lag $> p$ are all zero. In addition, assuming that the lag-l partial autoregressive matrix is zero, the likelihood ratio statistic $M(l)$ is asymptotically chi-squared distributed with four degrees of freedom. See Tiao and Box (1981) and Tsay (2014) for more details on properties of VARMA models.

For model identification, we employ the sample cross-correlation matrices (SCCM) and the likelihood ratio statistic $M(l)$ for the sample partial autoregressive matrices to help choose the appropriate orders p and q. Table 1 shows SCCM and the likelihood ratio statistic $M(l)$ for the series $\boldsymbol{\kappa}_t$. Since all SCCM of $\boldsymbol{\kappa}_t$ up to lag 8 are significantly not zero, we turn to the first-order difference $\Delta\boldsymbol{\kappa}_t$. Table 2 shows SCCM and $M(l)$ for $\Delta\boldsymbol{\kappa}_t$. Now only the lag-1 and lag-3 SCCM matrices are significantly not zero. We settle with the first-order difference. Since the critical value for $M(l)$ is $\chi^2_{4,0.95} = 9.45$, we see that $M(l)$ is significantly not zero at lags 1, 3 and 5 only. Based on these observations, we focus on VARMA(p, q) models with $p \leq 5$ and $q \leq 3$. Table 3 shows the Akaike Information Criterion (AIC) for different fitted VARMA models on $\Delta\boldsymbol{\kappa}_t$. VARMA$(5, 0)$ gives the lowest AIC which indicates that (5, 0) could be the best fitted model. The estimated coefficients and their corresponding standard errors of a VARMA$(5, 0)$ model fitted on $\Delta\boldsymbol{\kappa}_t$ are given in Table 4.

Tables 1–4 are here.

We then do diagnostic checking for the fitted VARMA$(5, 0)$ model. Table 5 shows the SCCM and $M(l)$ of the residuals after fitting a VARMA$(5, 0)$ model on $\Delta\boldsymbol{\kappa}_t$. SCCM matrices are insignificant from zero at all lags and $M(l)$ are all less than the critical value $\chi^2_{4,0.95} = 9.45$. We further check the normality assumption on errors since we are going to assume normality in simulation later. Table 6 shows the p-value and conclusion of normality tests on the residuals after fitting a VARMA$(5, 0)$ model on $\Delta\boldsymbol{\kappa}_t$. The residuals pass all the following three multivariate normality tests at 5% significance level: Royston's test, Henze–Zirkler's test, and Mardia's test.

Tables 5–6 are here.

In the end we want to point out that our choice of the VARMA$(5, 0)$ model for $\Delta\boldsymbol{\kappa}_t$ is consistent with the one chosen by Chan *et al.* (2014), who studied the CBD mortality indexes for England and Wales male population from 1950 to 2009.

2.3 Backtesting

The ex post forecasting performance of the fitted mortality model is important since reliable evaluation of CVA in K-forward would heavily depend on acceptable predictions of future mortality indexes that do not differ significantly from realized outcomes. Dowd *et al.* (2010) proposed a backtesting framework and applied it on a variety of stochastic mortality models. In particular, they investigated the out-of-sample predicting performance of the CBD mortality model by assuming that $\boldsymbol{\kappa}_t$ follows a bivariate random walk with drift. In the remaining of this section, we will perform similar backtesting under the assumption that $\Delta\boldsymbol{\kappa}_t$ follows a VARMA process.

According to Tsay (2014, Chapter 3), if a VARMA process (2.3) holds with $d = 1$, then $\Delta\boldsymbol{\kappa}_t$ has a moving-average representation

$$\Delta\boldsymbol{\kappa}_t = \boldsymbol{\mu} + \sum_{i=0}^{\infty} \Psi_i \boldsymbol{\epsilon}_{t-i},$$

where $\boldsymbol{\mu} = (\boldsymbol{I} - \Phi_1)^{-1}\Phi_0$, $\Psi_0 = \boldsymbol{I}$, $\Psi_1 = \Phi_1 - \Theta_1$, $\Psi_i = \Phi_1\Psi_{i-1}$, $i = 2, 3, \ldots$, and $\boldsymbol{I}$ is the 2×2 identity matrix. So we are able to derive

$$\boldsymbol{\kappa}_t = \boldsymbol{\kappa}_0 + \sum_{i=1}^{t} \Delta\boldsymbol{\kappa}_i = \boldsymbol{\kappa}_0 + t\boldsymbol{\mu} + \sum_{i=1}^{t}\sum_{j=0}^{t-i} \Psi_j \boldsymbol{\epsilon}_i + \sum_{i=0}^{\infty}\sum_{j=i+1}^{i+t} \Psi_j \boldsymbol{\epsilon}_{-i}.$$

Suppose that we are at time 0 and try to predict t steps ahead. Denote $\boldsymbol{\kappa}(t) = \mathrm{E}(\boldsymbol{\kappa}_t|\mathcal{F}_0)$ with $\mathcal{F}_0$ being the available information at time 0. Then,

$$\boldsymbol{\kappa}_t - \boldsymbol{\kappa}(t) = \sum_{i=1}^{t}\sum_{j=0}^{t-i} \Psi_j \boldsymbol{\epsilon}_i$$

and

$$\operatorname{cov}\left(\boldsymbol{\kappa}_t - \boldsymbol{\kappa}(t)\right) = \sum_{i=1}^{t} \left(\sum_{j=0}^{t-i} \Psi_j\right) \cdot \Sigma \cdot \left(\sum_{j=0}^{t-i} \Psi_j^{\top}\right).$$

Figure 3 shows the 95% prediction interval and median prediction line of $\kappa_t^{(1)}$ and $\kappa_t^{(2)}$ from 2000 to 2014 based on the mortality index data up to 1999. If the fitted model is proper, we would expect no more than 5% real mortality index turn out to fall outside of the confidence interval. It is clear that all real outcomes $\kappa_t^{(1)}$ from 2000 to 2014 fall within the interval. As for $\kappa_t^{(2)}$, only one out of fifteen real outcomes exceeds the interval boundary. Given that we have a relatively short forecast horizon (15 years), the ex post forecasting performance on both $\kappa_t^{(1)}$ and $\kappa_t^{(2)}$ is acceptable.

Figure 3 is here.

We also perform another backtest based on a formal statistical hypothesis test. Again we use the CBD mortality index data from 1933 to 1999. After fitting a VARMA(5,0) model on $\Delta\boldsymbol{\kappa}_t$, we can forecast by simulation the cumulative distribution function for $\kappa_t^{(1)}$ and $\kappa_t^{(2)}$ in future years. The null hypothesis is that the realized mortality indexes are consistent with their predicted distribution functions. Then by locating the realized $\kappa_t^{(i)}$, $i = 1, 2$, on its predicted distribution function curve, we can obtain its p-value, which is associated with the left-sided test of the null hypothesis. Note that here we focus on left-sided tests since if the model cannot generate adequate outcomes smaller than the realized $\kappa_t^{(i)}$, $i = 1, 2$, then it is not reliable to hedge longevity risk. The results are shown in Figure 4. It can be clearly seen that the model does a good job in predicting $\kappa_t^{(1)}$. Its p-values at all 15 horizon years are all greater than 10%. The p-value for $\kappa_t^{(2)}$ drops below 5% significance level only for the last two years in the forecast horizon. Given that $\kappa_t^{(1)}$ carries the main part of the longevity risk, as can be seen from the variations of $\kappa_t^{(i)}$, $i = 1, 2$, in Figure 2, the model has an acceptable performance in this backtest as well.

Figure 4 is here.

3 Risk-neutral default probability

In this section we employ a parametric reduced-form model to describe the default behaviour of a hedge provider. Given a set of non-callable bonds issued by the hedge provider, we try to match their "dirty prices" implied from the reduced-form model with their market prices. In this way we are able to determine the optimal set of parameters that gives us the best estimate for the hedge provider's risk-neutral default probability within a finite time horizon.

We assume that at time 0 the forward default intensity of the hedge provider is a deterministic positive function of time t, which has the form

$$h(t;\boldsymbol{\beta}) = \beta_0 + \beta_1 e^{-t/\beta_3} + \beta_2 e^{-t/\beta_3} t/\beta_3, \qquad t \geq 0, \tag{3.1}$$

with $\boldsymbol{\beta} = (\beta_0, \beta_1, \beta_2, \beta_3)^\mathsf{T} \in \mathbb{R}^4$. If $\boldsymbol{\beta}$ satisfies that $h(t;\boldsymbol{\beta}) > 0$ for all $t \geq 0$, then it is straightforward to derive the cumulative hazard rate function and the survival probability as

$$H(t;\boldsymbol{\beta}) = \frac{1}{t}\int_0^t h(s;\boldsymbol{\beta})\mathrm{d}s = \beta_0 + (\beta_1 + \beta_2)(1 - e^{-t/\beta_3})\beta_3/t - \beta_2 e^{-t/\beta_3} \tag{3.2}$$

and

$$S(t;\boldsymbol{\beta}) = \exp\left(-tH(t;\boldsymbol{\beta})\right), \quad t \geq 0. \tag{3.3}$$

The function $h(t;\boldsymbol{\beta})$ in (3.1) was first proposed by Nelson and Siegel (1987) to model a bond's yield curve. Duan *et al.* (2012) also found it useful in smoothing parameters when modeling forward default intensity. A great advantage of this parsimonious model is that all of the parameters have their own economic meanings. Indeed, β_0 is the long-term converging value of the default intensity, β_1 and β_2 represent the short-term and medium-term effects for the default intensity, respectively, and $\beta_3 > 0$ acts as the time-scalar parameter. In our application, since the default intensity is always positive, we require $S(t;\boldsymbol{\beta})$ in (3.3) to be a decreasing survival function, which means that, given $\boldsymbol{\beta}$,

$S(0;\boldsymbol{\beta}) = 1$, $\lim_{t\to\infty} S(t;\boldsymbol{\beta}) = 0$, and $S'(t;\boldsymbol{\beta}) < 0$ for all $t \geq 0$. Thus, besides $\beta_3 > 0$ we need the following additional constraints on $\boldsymbol{\beta}$:

(C1) $\beta_0 > 0$;
(C2) $\beta_0 + \beta_1 > 0$;
(C3) $\beta_2 > \beta_l$ with β_l uniquely satisfying $\beta_l < \beta_1$ and $\beta_0 + \beta_l \exp(\beta_1/\beta_l - 1) = 0$.

See Appendix A for the proof of the fact that constraints C1–C3 together is equivalent to that $S(t;\boldsymbol{\beta})$ is a decreasing survival function.

3.1 Model calibration

For a potential hedge provider, we estimate its risk-neutral forward default intensity by calibrating model (3.1) according to its available bond prices. Specifically, suppose we have detailed information, including market price, coupon rate, principal, maturity, etc., of K non-callable bonds issued by the hedge provider. The bond information is collected on the same day, which is considered as time 0. By combining discounted future coupon/principal payments with survival probability from (3.3), we are able to calculate the so-called "dirty price" for each bond as

$$\sum_{j=1}^{n} \mathrm{DF}(s_j) \cdot c\Delta_j \cdot S(s_j) + V \cdot \mathrm{DF}(s_n) \cdot S(s_n) + V \cdot R \cdot \int_0^{s_n} \mathrm{DF}(s) F(\mathrm{d}s). \tag{3.4}$$

In the above formula, $s_j, j = 1, \ldots, n$, are the coupon payment moments with s_n the maturity, c is the coupon rate, Δ_j is the fraction of years between s_{j-1} and s_j, V is the par value, R is the recovery rate, $\mathrm{DF}(\cdot)$ is the risk-free discount factor, $S(\cdot) = S(\cdot;\boldsymbol{\beta})$ for simplicity, and $F(\cdot) = 1 - S(\cdot)$. Note that in order to derive formula (3.4) we assume that the recovery is a fraction of the par value. Next we perform a calibration process on $\boldsymbol{\beta}$, under constraints C1–C3, such that the mean absolute error is minimized as

$$\boldsymbol{\beta}^* = \arg\min_{\boldsymbol{\beta}} \frac{1}{K} \sum_{k=1}^{K} \left| \text{dirty price}_k - \text{market price}_k \right|. \tag{3.5}$$

By doing so, we find for the hedge provider the optimal set of parameters $\boldsymbol{\beta}^*$ that best matches each bond's market price with its dirty price. Then we are able to use $h(t;\boldsymbol{\beta}^*)$ as the proxy for the hedge provider's risk-neutral forward default intensity.

We perform the model calibration process for two potential hedge providers: JP Morgan (JPM) and Royal Bank of Scotland (RBS), who have participated in transactions of longevity-linked securities in the last decade. See, for example, Table 1 of Biffis *et al.* (2016). The bond information of JPM and RBS, all retrieved on June 16, 2016 from Bloomberg database, is summarized in Tables 7–8, respectively.

Tables 7–8 are here.

Since all bonds are in US dollars, we use US Treasury zero yields on the same day to calculate the risk-free discount factor. Note that almost all of the bonds are senior unsecured except that two of RBS are subordinated. According to Table 24.2 of Hull (2014), the average recovery rate, as a percentage of par value, of senior unsecured corporate bonds in the period 1982–2012 is about 37%. Hence, we assume the fixed recovery rate $R = 37\%$ in the dirty price formula (3.4). We also want to point out that the optimization in (3.5) is nonlinear with multiple constraints, which is not trivial. We implement it in R 3.3.1 (R Core Team, 2016) using the NLopt package (Johnson, 2008).

The comparison of bonds' market prices and their dirty prices after model calibration is demonstrated in Figures 5–6. It is clear that the overall matching performance is very good with a mean absolute error of 0.496 dollars for JPM's ten bonds and of 0.923 dollars for RBS's seven bonds. Among all seventeen bonds, sixteen bonds have a percentage discrepancy less than 1.5% between dirty price and market price while there is only one exception at 4.5%.

Figures 5–6 are here.

We also look at the estimated risk-neutral credit spread term structure of the two banks. Here the credit spread at time t is simply defined as $(1 - R)H(t; \boldsymbol{\beta})$. The left plot in Figure 7 displays JPM's credit spread term structure estimated by assuming $\boldsymbol{\beta} = \boldsymbol{\beta}^*_{\text{JPM}} = (0.0125, 0.0050, 0.0181, 2.8895)^\intercal$. The credit spread curve is hump shaped, increasing up to around 5 years and then keeping decreasing beyond that point. This is a generic B-rating credit spread curve according to Lando and Mortensen (2005). Similarly, the right plot in Figure 7 displays RBS's credit spread term structure estimated by assuming $\boldsymbol{\beta} = \boldsymbol{\beta}^*_{\text{RBS}} = (0.0210, 0.0170, 0.0676, 4.9448)^\intercal$. Again, the credit spread curve is hump shaped with the peak at around the 5-year point. But compared with that of JPM, the credit spread curve of RBS clearly shifts to a much higher level.

Figure 7 is here.

So we find something interesting here. According to Moody's, JPM's senior unsecured bonds are rated at A3 in the category of medium grade and RBS's senior unsecured bonds are rated at Ba1 in the category of non-investment grade speculative. However, their risk-neutral credit spread curves, estimated based on their public-traded bonds, both behave like a B-rating one, which belongs to the highly speculative category. This indicates that the financial market is very risk averse when pricing credit risk.

4 CVA of K-forward

In this section we calculate CVA of K-forwards for a pension fund. We assume that the pension fund and a hedge provider have an agreement of K-forwards written on US male population as described in Section 2. The two potential hedge providers we consider in this paper are JPM and RBS. We use the CVA evaluation formula (1.1), in which the risk exposures are calculated by applying the vector time-series model on the CBD mortality indexes $\boldsymbol{\kappa}_t$ as in Section 2 and the risk-neutral default probability is estimated by calibrating the reduced-form model on the hedge provider's bond prices as in Section 3. Next we state the assumptions and steps of our calculation before we present the numerical results in Section 4.1.

We assume time 0 as on June 16, 2016, on which date we collected bonds' information for the two potential hedge providers. The K-forwards are used to hedge longevity risk for up to 25 years beyond 2016. Denote by $\boldsymbol{\kappa}_0$ the mortality indexes of year 2016, by $\boldsymbol{\kappa}_1$ the mortality indexes of year 2017, and so on. In practice, there is usually a time lag between the end of a reference year and the availability of the mortality index data for that year. For simplicity, we suppose in this paper that $\boldsymbol{\kappa}_t$ for each year starting 2016 are available on December 31 of the same year. At the end of each year t we can obtain an updated estimate of $\boldsymbol{\kappa}_T$ by applying the fitted VARMA model to the realization of $\boldsymbol{\kappa}_t$ up to year t. We then plug the updated estimates of $\boldsymbol{\kappa}_T$ in formula (2.2) to get the risk exposures of the K-forwards at year t. The CVA is an accumulation up to year T of the discounted risk exposure combined with the default probability and the loss given default. The detailed simulation procedure is as follows:

Step 1: Simulate a sample path of $\boldsymbol{\kappa}_t, t = 0, 1, \ldots, T$, based on the historical mortality indexes $\boldsymbol{\kappa}_t$ and the fitted VARMA(5, 0) model on $\Delta\boldsymbol{\kappa}_t$.

Step 2: At the end of each year $t = 0, 1, \ldots, T$, update the estimate of $\boldsymbol{\kappa}_T$ based on the simulations up to year t from Step 1. Compare it with the original value estimated at time 0 to determine the risk exposure at that point.

Step 3: For each risk exposure at the end of year t in Step 2, multiply it with the marginal risk-neutral default probability in year t, the risk-free discount factor corresponding to the end of year t, and the loss given default.

Step 4: A realization of CVA is obtained by adding together all the products for years $t = 0, 1, \ldots, T$, in Step 3.

Step 5: Repeat Steps 1–4 for 1,000,000 times. The average CVA is our final estimate.

4.1 Numerical results

The numerical results of CVA measured in basis points (bpts) for K1-forward and K2-forward are summarized in Table 9.

Table 9 is here.

Our first observation is that for US male population the CVA of K1-forward is always much larger than that of K2-forward. For instance, the CVA of K1-forward at $T = 25$ years is 52.4 bpts for JPM, more than half of the corresponding credit spread (95.4 bpts), while the CVA of K2-forward for the same reference year is only 1.6 bpts, which is almost negligible. The big discrepancy in CVA values is actually due to the fact that $\kappa_t^{(1)}$ measures the level of the whole logit-transformed mortality curve while $\kappa_t^{(2)}$ represents the slope of the logit-transformed mortality curve. In Figure 2 we can easily see that for US male population the fluctuation in $\kappa_t^{(1)}$ contains the main part of the longevity risk and bears a larger uncertainty along with time. It would be interesting to know if this relationship between K1-forward and K2-forward holds for other populations as well given that some populations, like Canadian male as found by Chan *et al.* (2014), may have relatively less uncertainty associated with $\kappa_t^{(1)}$ but more uncertainty associated with $\kappa_t^{(2)}$.

Second, the CVA of K-forward is greatly influenced by the hedge provider's credit rating. As we introduced in Section 3, the long-term credit rating of JPM is A3, which belongs to the category of medium grade, while that of RBS is Ba1, which is in the category of non-investment grade speculative. As a result, the credit spreads of RBS at years 15, 20 and 25 are all as about two and a half times as that of JPM. Similarly, for both K1-forward and K2-forward, CVA of RBS is almost as double as that of JPM. The different levels of scaling confirm that CVA, unlike credit spread which is the risk premium for a specific time point, depends essentially on the whole credit curve of the hedge provider. This also makes it very important to accurately estimate the whole credit curve, not only credit spreads at some time points, in order to obtain a reliable estimate of CVA.

Last we want to talk about the impact of recovery rate. We fix the recovery rate at 37% in the above calculation only because it is the historically average recovery rate of senior unsecured corporate bonds. But in reality the recovery rate is not known at issuance and its realized value could be any number between 0 and 1. We calculate the CVAs again by assuming that financial market believes the hedge provider might default with a recovery rate of 25% and 50%, respectively. The results are summarized in Tables 10–11. It can be clearly seen that the randomness of recovery rate has a big impact on CVA for a hedge provider with non-investment grade, like RBS. For instance, when the assumed recovery rate drops from 50% to 37%, corresponding to a 26% increase of LGD, the CVA of K1-forward at year 25 for RBS increases by 33.8%!

Tables 10–11 are here.

5 Concluding remarks

In this paper, we propose a baseline framework to calculate CVA in K-forward. The risk exposure part is obtained by applying a VARMA model on mortality indexes. The risk-neutral default probability is derived from a reduced-form model that is calibrated according to market bond prices. This framework works for arbitrary combination of hedge provider, reference year and recovery rate.

One way to extend our work is to take into account recovery risk. One possible solution is to use a structural model with downward jumps to describe the default behaviour of the hedge provider. It is natural to relate the recovery rate to the random default severity. Another advantage of using a structural model is that we are able to compare results under two different default models and figure out if there is severe model risk in the evaluation of CVA.

Another issue that we need to consider in future research is debt value adjustment (DVA) from the hedger's perspective. In other words, we need to consider the possibility that the hedger defaults before the hedge provider does, which may causes potential losses for the hedge provider. Since hedge providers of K-forward are usually banks, who are required by regulation to report CVA of OTC derivatives in their financial statements, it is important to consider CVA and DVA in K-forward together.

References

[1] Biffis, E.; Blake., D.; Pitotti, L.; Sun, A. (2016). The cost of counterparty risk and collateralization in longevity swaps. *Journal of Risk and Insurance* **83**, no. 2, 387–419.

[2] Blake, D.; Cairns, A.; Coughlan, G.; Dowd, K.; MacMinn, R. (2013). The new life market. *Journal of Risk and Insurance* **80**, no. 3, 501–558.

[3] Blake, D.; Cairns, A.; Dowd, K. (2006). Living with mortality: Longevity bonds and other mortality-linked securities. *British Actuarial Journal* **12**, no. 1, 153–197.

[4] Cairns, A.; Blake., D.; Dowd, K. (2006). A two-factor model for stochastic mortality with parameter uncertainty: theory and calibration. *Journal of Risk and Insurance* **73**, no. 4, 687–718.

[5] Cairns, A.; Blake., D.; Dowd, K.; Coughlan, G.; Epstein, D.; Khalaf-Allah, M. (2011). Mortality density forecasts: an analysis of six stochastic mortality models. *Insurance: Mathematics and Economics* **48**, no. 3, 355–367.

[6] Cairns, A.; Dowd, K.; Blake, D.; Coughlan, G. (2014). Longevity hedge effectiveness: A decomposition. *Quantitative Finance* **14**, no. 2, 217–235.

[7] Chan, W.; Li, J.; Li, J. (2014). The CBD mortality indexes: modeling and applications. *North American Actuarial Journal* **18**, no. 1, 38–58.

[8] Coughlan, G; Epstein, D.; Sinha, A.; Honig, P. (2007). q-forwards: Derivatives for transferring longevity and mortality risks. *JPMorgan Pension Advisory Group*, London.

[9] Cox, S.H.; Pedersen, H.W. (2000). Catastrophe risk bonds. *North American Actuarial Journal* **4**, no. 4, 56–82.

[10] Dowd, K.; Cairns, A.; Blake, D.; Coughlan, G.; Epstein, D.; Khalaf-Allah, M. (2010). Backtesting stochastic mortality models: an ex post evaluation of multiperiod-ahead density forecasts. *North American Actuarial Journal* **14**, no. 3, 281–298.

[11] Duan, J.-C.; Sun, J.; Wang, T. (2012). Multiperiod corporate default prediction – a forward intensity approach. *Journal of Econometrics* **170**, no. 1, 191–209.

[12] Gregory, J. (2015). *The XVA Challenge: Counterparty Credit Risk, Funding, Collateral and Capital*. John Wiley & Sons.

[13] Hull, J. (2014). *Options, Futures, and Other Derivatives*, 9th edition. Pearson Education.

[14] Human Mortality Database. (2016). University of California, Berkeley, USA, and Max Planck Institute for Demographic Research, Germany. Available at www.mortality.org.

[15] Hunt, A.; Blake, D. (2015). Modelling longevity bonds: Analysing the Swiss Re Kortis Bond. *Insurance: Mathematics and Economics* **63**, 12–29.

[16] Johnson, S.G. (2008). The NLopt nonlinear-optimization package. URL http://ab-initio.mit.edu/nlopt/.

[17] Lando, D.; Mortensen, A. (2005). Revisiting the slope of the credit spread curve. *Journal of Investment Management* **3**, no. 4, 1–27.

[18] Li, J.; Chan, W.; Cheung, S. (2011). Structural changes in the Lee-Carter mortality indexes. *North American Actuarial Journal* **15**, no. 1, 13–31.

[19] Nelson, C.R.; Siegel, A.F. (1987). Parsimonious modeling of yield curves. *Journal of Business* **60**, no. 4, 473–489.

[20] R Core Team (2016). R: A language and environment for statistical computing. R Foundation for Statistical Computing, Vienna, Austria. URL http://www.R-project.org.

[21] Tan, C.; Li, J.; Li, J.; Balasooriya, U. (2014). Parametric mortality indexes: From index construction to hedging strategies. *Insurance: Mathematics and Economics* **59**, 285–299.

[22] Tiao, G.; Box, G. (1981). Modeling multiple time series with applications. *Journal of the American Statistical Association* **76**, no. 376, 802–816.

[23] Tsay, R. (2014). *Multivariate Time Series Analysis: With R and Financial Applications*. John Wiley & Sons.

Appendix A

Here we give the proof of the fact that the combination of constraints C1–C3 on $\boldsymbol{\beta}$, as given in Section 3, is equivalent to that $S(t;\boldsymbol{\beta})$ is a decreasing survival function.

Actually by (3.2), for $t > 0$,

$$tH(t,\boldsymbol{\beta}) = t\beta_0 + (\beta_1+\beta_2)(1-e^{-t/\beta_3})\beta_3 - t\beta_2 e^{-t/\beta_3}.$$

It is obvious that $\lim_{t\to 0^+} tH(t,\boldsymbol{\beta}) = 0$ and thus we always have $S(0;\boldsymbol{\beta}) = 1$. Since $\beta_3 > 0$, by (3.3), we have

$$\begin{aligned}\lim_{t\to\infty} S(t;\boldsymbol{\beta}) = 0 &\iff \lim_{t\to\infty} tH(t;\boldsymbol{\beta}) = \infty \\ &\iff \lim_{t\to\infty} t\beta_0 + (\beta_1+\beta_2)\beta_3 = \infty \\ &\iff \beta_0 > 0,\end{aligned}$$

which is constraint C1.

Then, with $\beta_0 > 0$ and $\beta_3 > 0$, we prove that $S'(t;\boldsymbol{\beta}) < 0$ for all $t \geq 0$ is equivalent with constraints C2 and C3. It is obvious that

$$S'(t;\boldsymbol{\beta}) < 0, \forall t \geq 0 \iff h(t;\boldsymbol{\beta}) > 0, \forall t \geq 0. \tag{A.1}$$

Since $h(0;\boldsymbol{\beta}) = \beta_0 + \beta_1$ and $\lim_{t\to\infty} h(t;\boldsymbol{\beta}) = \beta_0$, from (A.1) we immediately have $\beta_0 + \beta_1 > 0$, which is constraint C2. Given $\beta_0 > 0$, $\beta_0 + \beta_1 > 0$ and $\beta_3 > 0$, we next derive the constraint on β_2. Note that $h(t;\boldsymbol{\beta})$ is a smooth function on $[0,\infty)$ with

$$h'(t;\boldsymbol{\beta}) = (\beta_2 - \beta_1 - t\beta_2/\beta_3)\cdot \exp\left(-t/\beta_3\right)/\beta_3.$$

It is straightforward to see that when $\beta_2 \geq \min(0,\beta_1)$, $h(t;\boldsymbol{\beta})$ takes its infimum of $\beta_0 + \beta_1$ ($t = 0$) or of β_0 ($t = \infty$), both greater than zero. While, when $\beta_2 < \min(0,\beta_1)$, $h'(t;\boldsymbol{\beta})$ has a unique root $t^* = \beta_3(1-\beta_1/\beta_2) \in (0,\infty)$ and $h(t;\boldsymbol{\beta})$ takes its infimum of $h(t^*;\boldsymbol{\beta}) = \beta_0 + \beta_2 \exp(\beta_1/\beta_2 - 1)$. Denote by β_l the unique value satisfying $\beta_l < \beta_1$ and $\beta_0 + \beta_l \exp(\beta_1/\beta_l - 1) = 0$. Then $h(t^*;\boldsymbol{\beta}) > 0$ requires $\beta_2 > \beta^*$. So we have $h(t;\boldsymbol{\beta}) > 0, \forall t \geq 0$, implies $\beta_2 > \beta_l$, which is constraint C3. It is also easy to check that, with $\beta_0 > 0$ and $\beta_3 > 0$, constraints C2 and C3 together implies the condition in (A.1). The proof is completed.

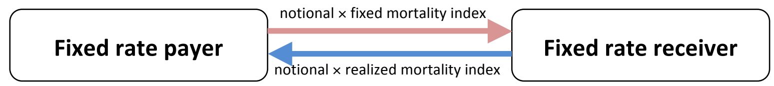

Figure 1: The transaction between two parties of a K-forward

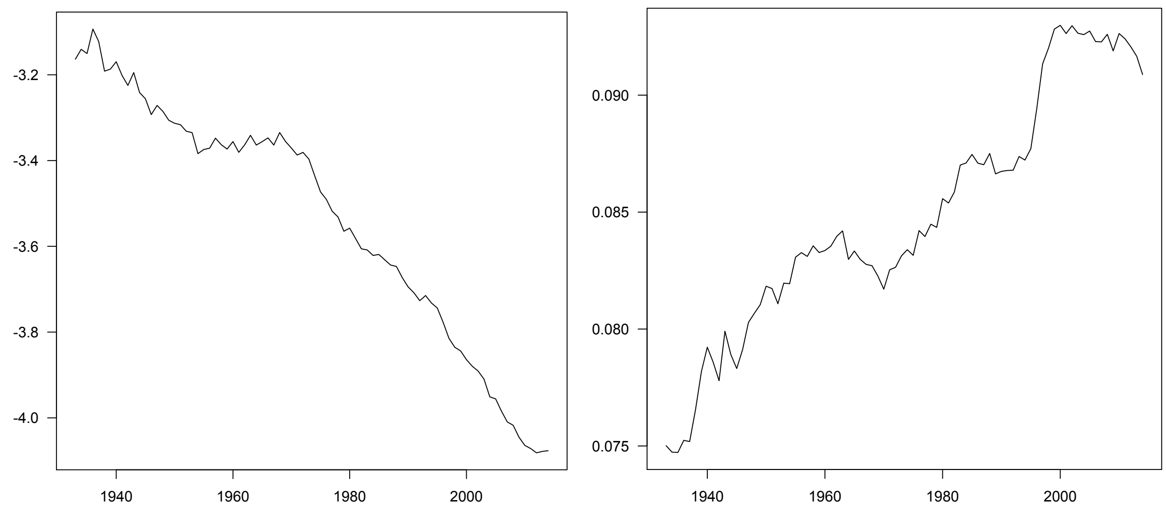

Figure 2: Historical values of $\kappa_t^{(1)}$ (left panel) and $\kappa_t^{(2)}$ (right panel) for US male population aged from 30 to 100, 1933–2014

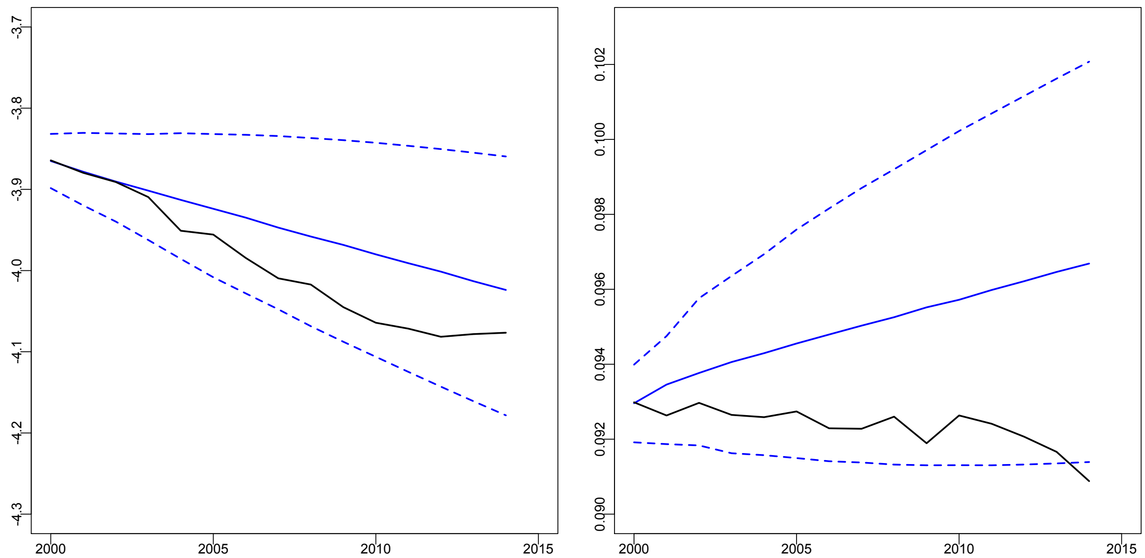

Figure 3: The 95% prediction interval and median line of $\kappa_t^{(1)}$ (left panel) and $\kappa_t^{(2)}$ (right panel) in 2000–2014 based on the mortality index data up to 1999. The dashed lines represent lower and upper bounds of the confidence interval, the blue continuous line represents the forecasted median, and the black continuous line represents the real outcome of the mortality index.

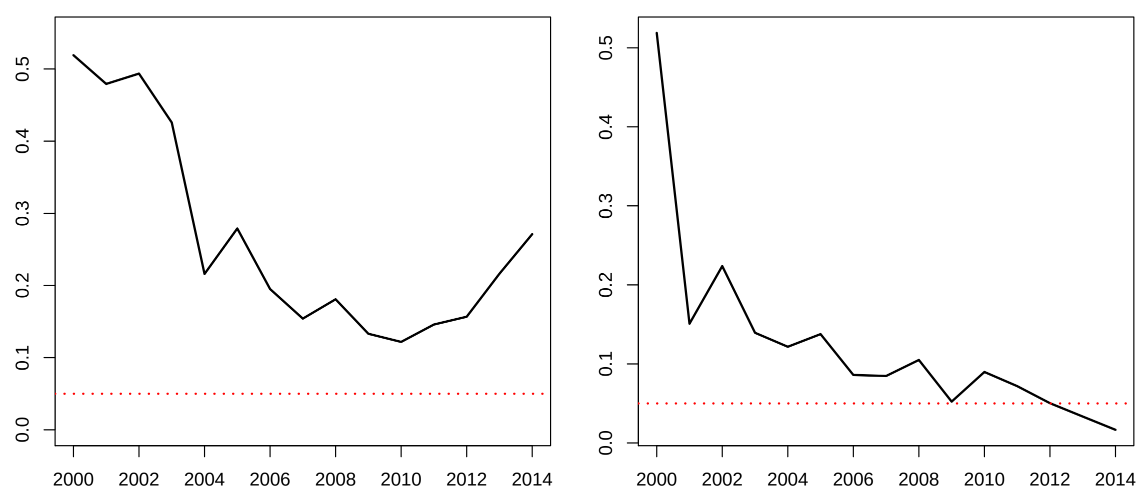

Figure 4: The various-horizon p-values of realized $\kappa_t^{(1)}$ (left panel) and $\kappa_t^{(2)}$ (right panel) in 2000–2014 based on the mortality index data up to 1999. The red dotted line represents the 5% significance level.

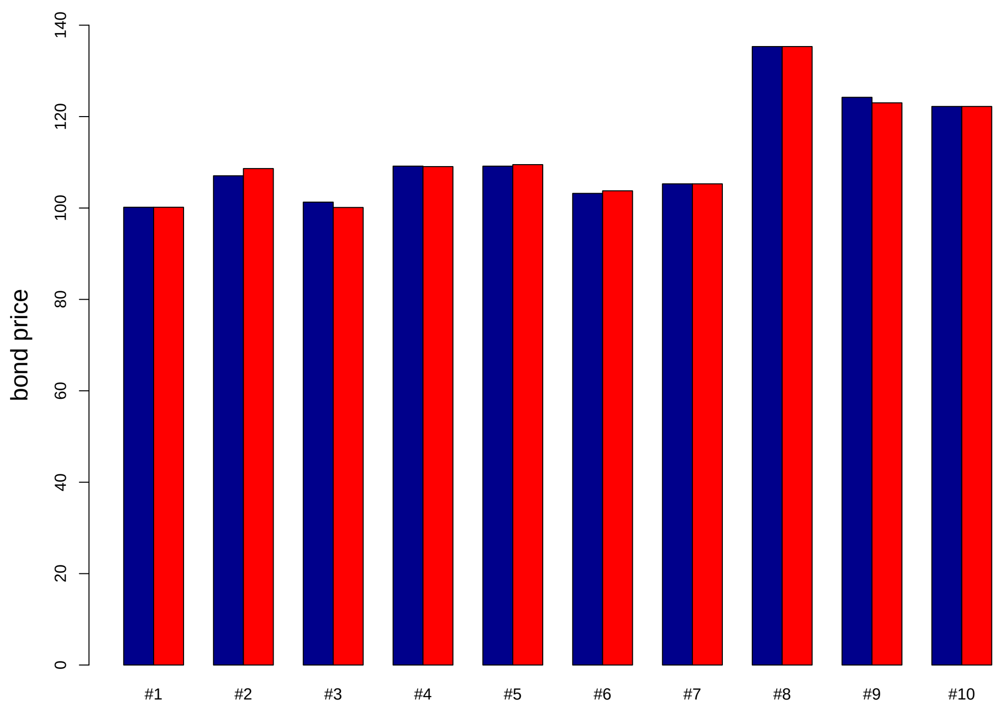

Figure 5: Calibration results for JPM. The blue bars represent bonds' market prices and the red bars represent bonds' dirty prices with $\boldsymbol{\beta}^*_{\text{JPM}} = (0.0125, 0.0050, 0.0181, 2.8895)^\mathsf{T}$. The mean absolute error is 0.496.

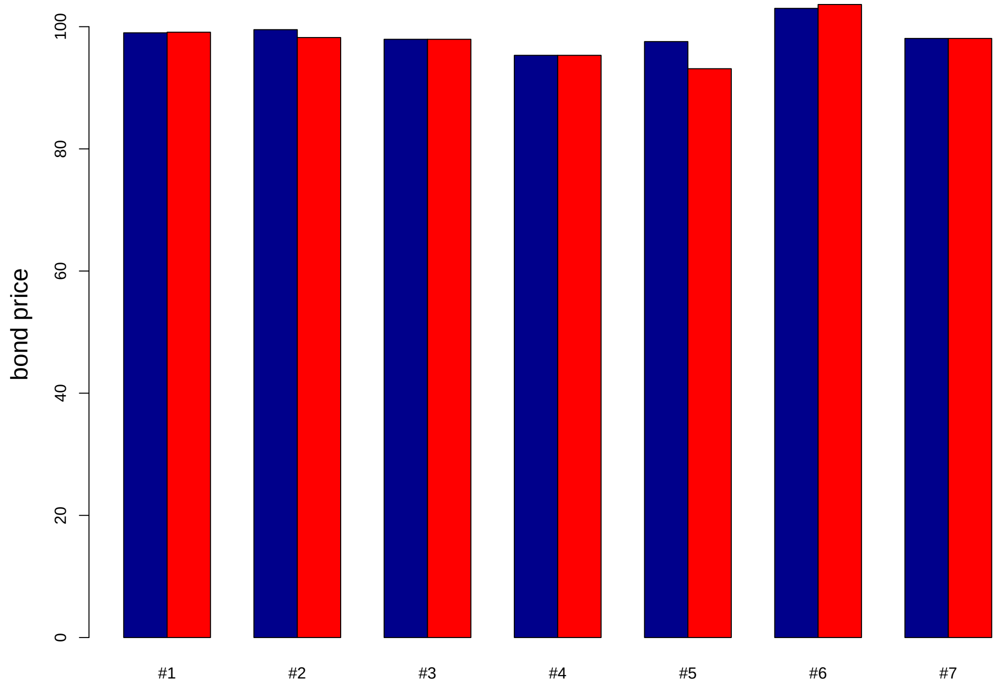

Figure 6: Calibration results for RBS. The blue bars represent bonds' market prices and the red bars represent bonds' dirty prices with $\boldsymbol{\beta}^*_{\text{RBS}} = (0.0210, 0.0170, 0.0676, 4.9448)^\mathsf{T}$. The mean absolute error is 0.923.

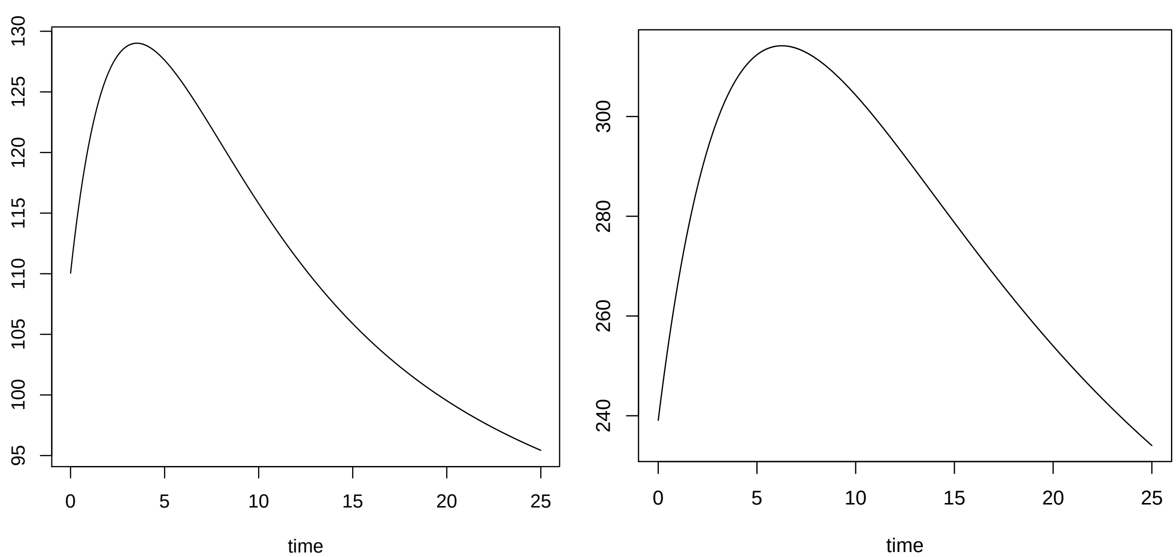

Figure 7: Estimated credit spread term structure of JPM (left panel) and RBS (right panel) on June 16, 2016

Table 1: Sample cross-correlation matrices and likelihood ratio statistics of $\boldsymbol{\kappa}_t$

	lag l							
	1	2	3	4	5	6	7	8
SCCM	$\begin{bmatrix} + & - \\ - & + \end{bmatrix}$	$\begin{bmatrix} + & - \\ - & + \end{bmatrix}$	$\begin{bmatrix} + & - \\ - & + \end{bmatrix}$	$\begin{bmatrix} + & - \\ - & + \end{bmatrix}$	$\begin{bmatrix} + & - \\ - & + \end{bmatrix}$	$\begin{bmatrix} + & - \\ - & + \end{bmatrix}$	$\begin{bmatrix} + & - \\ - & + \end{bmatrix}$	$\begin{bmatrix} + & - \\ - & + \end{bmatrix}$
$M(l)$	490.39	22.05	5.62	16.27	2.68	11.53	5.18	-0.45

Table 2: Sample cross-correlation matrices and likelihood ratio statistics of $\Delta\boldsymbol{\kappa}_t$

	lag l							
	1	2	3	4	5	6	7	8
SCCM	$\begin{bmatrix} \cdot & \cdot \\ - & \cdot \end{bmatrix}$	$\begin{bmatrix} \cdot & \cdot \\ \cdot & \cdot \end{bmatrix}$	$\begin{bmatrix} \cdot & \cdot \\ + & \cdot \end{bmatrix}$	$\begin{bmatrix} \cdot & \cdot \\ \cdot & \cdot \end{bmatrix}$	$\begin{bmatrix} \cdot & \cdot \\ \cdot & \cdot \end{bmatrix}$	$\begin{bmatrix} \cdot & \cdot \\ \cdot & \cdot \end{bmatrix}$	$\begin{bmatrix} \cdot & \cdot \\ \cdot & \cdot \end{bmatrix}$	$\begin{bmatrix} \cdot & \cdot \\ \cdot & \cdot \end{bmatrix}$
$M(l)$	19.89	1.96	18.57	6.48	14.13	5.14	-0.13	-0.78

Table 3: AIC of fitted VARMA(p,q) models on $\Delta\boldsymbol{\kappa}_t$

(p,q)	(5,0)	(4,0)	(3,0)	(2,0)	(1,0)	(0,1)	(0,2)	(0,3)
AIC	-22.827	-22.719	-22.707	-22.517	-22.600	-22.581	-22.559	-22.792

Table 4: Coefficients and their standard errors of a VARMA$(5,0)$ model fitted on $\Delta\boldsymbol{\kappa}_t$

Φ_0	Φ_1	Φ_2
$\begin{pmatrix} \begin{matrix}-0.0080\\(0.0035)\end{matrix} \\ \\ \begin{matrix}-0.000050\\(0.000113)\end{matrix} \end{pmatrix}$	$\begin{pmatrix} \begin{matrix}-0.0889\\(0.1086)\end{matrix} & \begin{matrix}-6.1141\\(3.5450)\end{matrix} \\ \\ \begin{matrix}-0.0175\\(0.0034)\end{matrix} & \begin{matrix}0.0273\\(0.1127)\end{matrix} \end{pmatrix}$	$\begin{pmatrix} \begin{matrix}0.0010\\(0.1222)\end{matrix} & \begin{matrix}0.6678\\(3.5310)\end{matrix} \\ \\ \begin{matrix}-0.0098\\(0.0039)\end{matrix} & \begin{matrix}0.1542\\(0.1118)\end{matrix} \end{pmatrix}$
Φ_3	Φ_4	Φ_5
$\begin{pmatrix} \begin{matrix}0.1451\\(0.1142)\end{matrix} & \begin{matrix}0.2323\\(3.4340)\end{matrix} \\ \\ \begin{matrix}0.0086\\(0.0036)\end{matrix} & \begin{matrix}0.1308\\(0.1090)\end{matrix} \end{pmatrix}$	$\begin{pmatrix} \begin{matrix}0.1672\\(0.1177)\end{matrix} & \begin{matrix}1.9997\\(3.3920)\end{matrix} \\ \\ \begin{matrix}0.0066\\(0.0037)\end{matrix} & \begin{matrix}-0.0632\\(0.1076)\end{matrix} \end{pmatrix}$	$\begin{pmatrix} \begin{matrix}0.0817\\(0.1167)\end{matrix} & \begin{matrix}1.0612\\(3.0140)\end{matrix} \\ \\ \begin{matrix}-0.0006\\(0.0037)\end{matrix} & \begin{matrix}0.0345\\(0.0956)\end{matrix} \end{pmatrix}$
Σ		
$\begin{pmatrix} 0.00027272 & 0.00000199 \\ 0.00000199 & 0.00000027 \end{pmatrix}$		

Table 5: Sample cross-correlation matrices and likelihood ratio statistics of the residuals after fitting a VARMA$(5,0)$ model on $\Delta\boldsymbol{\kappa}_t$

	lag l							
	1	2	3	4	5	6	7	8
	SCCM							
	$\begin{bmatrix} \cdot & \cdot \\ \cdot & \cdot \end{bmatrix}$	$\begin{bmatrix} \cdot & \cdot \\ \cdot & \cdot \end{bmatrix}$	$\begin{bmatrix} \cdot & \cdot \\ \cdot & \cdot \end{bmatrix}$	$\begin{bmatrix} \cdot & \cdot \\ \cdot & \cdot \end{bmatrix}$	$\begin{bmatrix} \cdot & \cdot \\ \cdot & \cdot \end{bmatrix}$	$\begin{bmatrix} \cdot & \cdot \\ \cdot & \cdot \end{bmatrix}$	$\begin{bmatrix} \cdot & \cdot \\ \cdot & \cdot \end{bmatrix}$	$\begin{bmatrix} \cdot & \cdot \\ \cdot & \cdot \end{bmatrix}$
$M(l)$	-1.09	1.08	-1.25	2.64	7.04	2.44	4.74	5.27

Table 6: Normality tests on the residuals after fitting a VARMA$(5,0)$ model on $\Delta\boldsymbol{\kappa}_t$

Test	p-value	Conclusion
Shapiro–Wilk for $\Delta\kappa^{(1)}$	0.409	pass
Shapiro–Wilk for $\Delta\kappa^{(2)}$	0.149	pass
Royston's	0.251	pass
Henze–Zirkler's	0.391	pass
Mardia's	N.A.	pass

Table 7: Ten bonds of JP Morgan on June 16, 2016

Maturity	Par	Coupon	Frequency	Last price	Currency	Type
0.668	100.000	1.350	semiannually	100.166	USD	Senior secured
1.584	100.000	6.000	semiannually	107.050	USD	Senior secured
3.351	100.000	2.200	semiannually	101.290	USD	Senior secured
4.101	100.000	4.400	semiannually	109.164	USD	Senior secured
5.167	100.000	4.350	semiannually	109.158	USD	Senior secured
6.614	100.000	3.200	semiannually	103.199	USD	Senior secured
7.912	100.000	3.625	semiannually	105.290	USD	Senior secured
21.926	100.000	6.400	semiannually	135.326	USD	Senior secured
24.348	100.000	5.500	semiannually	124.220	USD	Senior secured
25.575	100.000	5.400	semiannually	122.221	USD	Senior secured

Table 8: Seven bonds of Royal Bank of Scotland on June 16, 2016

Maturity	Par	Coupon	Frequency	Last price	Currency	Type
1.249	100.000	2.650	monthly	99.000	USD	Senior secured
1.499	100.000	2.250	monthly	99.513	USD	Senior secured
1.668	100.000	2.150	monthly	97.938	USD	Senior secured
3.668	100.000	2.750	monthly	95.313	USD	Senior secured
6.501	100.000	3.650	monthly	97.563	USD	Senior secured
6.986	100.000	6.100	semiannually	103.000	USD	Subordinated
7.926	100.000	5.125	semiannually	98.076	USD	Subordinated

Table 9: CVA (in bpts) of K-forwards when $R = 0.37$ with standard errors in parenthesis

	$T = 15$			$T = 20$			$T = 25$		
	K1	K2	sprd	K1	K2	sprd	K1	K2	sprd
JPM	34.2	1.1	105.9	43.9	1.4	99.5	52.4	1.6	95.4
	(.10)	(.004)		(.13)	(.005)		(.15)	(.006)	
RBS	73.4	2.3	278.7	87.7	2.7	254.0	97.8	3.0	234.0
	(.23)	(.008)		(.26)	(.009)		(.28)	(.010)	

Table 10: CVA (in bpts) of K-forwards when $R = 0.25$ with standard errors in parenthesis

	$T = 15$			$T = 20$			$T = 25$		
	K1	K2	sprd	K1	K2	sprd	K1	K2	sprd
JPM	35.8	1.1	109.8	47.5	1.5	106.0	58.0	1.8	103.8
	(.11)	(.004)		(.14)	(.005)		(.16)	(.006)	
RBS	80.6	2.5	293.3	95.4	2.9	262.5	104.2	3.2	233.0
	(.25)	(.009)		(.28)	(.010)		(.30)	(.011)	

Table 11: CVA (in bpts) of K-forwards when $R = 0.50$ with standard errors in parenthesis

	$T = 15$			$T = 20$			$T = 25$		
	K1	K2	sprd	K1	K2	sprd	K1	K2	sprd
JPM	29.7	0.9	95.2	37.4	1.2	87.8	44.1	1.4	83.2
	(.09)	(.003)		(.11)	(.004)		(.12)	(.005)	
RBS	60.4	1.9	242.2	68.4	2.1	206.6	73.1	2.2	179.0
	(.19)	(.007)		(.20)	(.007)		(.21)	(.008)	